INVESTIGATING SULFUR-RICH MERCURY ANALOGS EXPOSED TO SIMULATED MICROMETEOROID BOMBARDMENT IN THE LABORATORY. N. Bott[1], M. S. Thompson[1], M. J. Loeffler[2], K. B. Prissel[3], K. E. Vander Kaaden[4] and F. M. McCubbin[5], [1]Department of Earth, Atmospheric, and Planetary Sciences, Purdue University, West Lafayette, IN, 47907, USA (nbott@purdue.edu), [2]Northern Arizona University, Flagstaff, AZ, 86011, USA, [3]Jacobs, NASA Johnson Space Center, Houston, TX, 77058, USA, [4]NASA Headquarters, Mary W. Jackson Building, Washington, DC, 20546, USA, [5]ARES, NASA Johnson Space Center, Houston, TX, 77058, USA.

Introduction: Space weathering (SW) continually alters the spectral, microstructural, and chemical characteristics of the surface of airless bodies across the solar system [1]. The effects of SW vary depending on the heliocentric distance and the initial composition of the target surface [2]. While SW on the Moon and S-type asteroids is well documented, our understanding of how this process affects Mercury is at an early stage. Mercury's interplanetary environment is harsh, with the surface of the planet experiencing an intense solar wind flux as well as a higher flux and velocity of micrometeoroid impactors compared to the Moon and S-type asteroids [3]. In addition, Mercury is also a geochemical endmember, with a surface composition low in Fe (<2 wt.%) [4] and enriched in volatile components, such as sulfur (up to 4 wt.% in the low reflectance material (LRM)) [4,5]. These volatile components are thought to play a major role in the formation of hollows via their sublimation [6,7].

Sulfur has been hypothesized to occur at the surface of Mercury as sulfide minerals (MgS, CaS) based on its correlation with Mg and Ca in remote sensing data [8]. However, recent observations of chaotic terrains in the north polar area of Mercury and of glacier-like features at lower latitudes indicated that octasulfur (S_8, elemental sulfur) is another likely constituent of a volatile-rich layer in Mercury's crust [9]. Its behavior on Mercury may result in a complex cycle of enrichment and depletion. While S is often depleted on small body surfaces [10], Mercury's gravity could result in ejected S subsequently returning to the surface and coating regolith grains. Further, the reaction of reduced S-rich gas with glasses of a Mercury-like composition also produced S-rich coatings [11]. However, the precise behavior and evolution of S-rich species exposed to the harsh SW on Mercury remains poorly understood and needs to be further investigated in the laboratory.

Here, we present the results of our analyses of the spectral, microstructural, and chemical characteristics of S-rich Mercury analogs irradiated by pulsed laser to simulate the short duration, high temperature events associated with micrometeoroid impacts.

Samples and Methods: We synthetized three powdered samples (grain size: 45-125 µm) of forsteritic olivine at NASA Johnson Space Center (JSC) [12]. All samples have low FeO contents, consistent with those observed at the surface of Mercury: F-T-004 (0.53 wt.% FeO), F-T-002 (0.1 wt.% FeO) and F-S-002 (0.05 wt.% FeO). We mixed our samples with sulfur at 4 wt.% to account for its highest observed concentration on Mercury, in particular in the LRM [7]. The mixtures were pressed into pellets at Northern Arizona University (NAU). Similar to previous mixtures with graphite [12], the pellets were irradiated with a Nd-YAG (λ=1064 nm) pulsed laser under ultra-high vacuum to simulate progressive exposure to micrometeoroid impacts. In addition, we suspended a Si wafer next to the samples to collect any vapor or melt deposits ejected from the surface of the sample during the irradiation.

Ex situ UV-visible (0.25-0.9 µm) reflectance spectra of the samples were acquired using an Avantes 2048XL fiber optic spectrometer, and both *ex situ* and *in situ* near-infrared (0.75-2.5 µm) reflectance spectra were acquired using a Nicolet IS50 FTIR spectrometer at NAU. The surface morphology of the samples was analyzed by scanning electron microscopy (SEM) using a Hitachi TM 4000 Plus benchtop SEM equipped with Oxford energy dispersive x-ray (EDX) detectors at Purdue University. Lastly, electron-transparent thin sections of the samples were prepared with a Thermo Scientific Helios G4 UX DualBeam focused ion beam (FIB) for analysis with the FEI Talos 200X transmission electron microscope (TEM) equipped with a Super-X EDX detector at Purdue.

Results and Discussion:

Reflectance spectroscopy: For all samples, the most significant spectral differences occur after 1 laser raster (Figure 1). We observe a global reddening and a decrease in the 1 µm absorption band depth with progressive irradiation, for all samples. We also note a clear brightening after irradiation for sample F-S-002, indicating there is a threshold of Fe content (between 0.1 and 0.05 wt.%) below which laser irradiation produces brightening, and not darkening. Interestingly, a similar behavior was observed for irradiated mixtures with graphite, but with a different threshold of Fe content [12]. Finally, we notice the NIR slope (1.75-2.5 µm) depends on the Fe content – the higher the Fe content, the redder the NIR slope.

Electron Microscopy: We identified melt deposits on forsterite grains in the irradiated region of the samples. A few sulfur-rich deposits are also observed across the irradiated pellets (Figure 2). No elemental S particles can be found at the surface of the samples

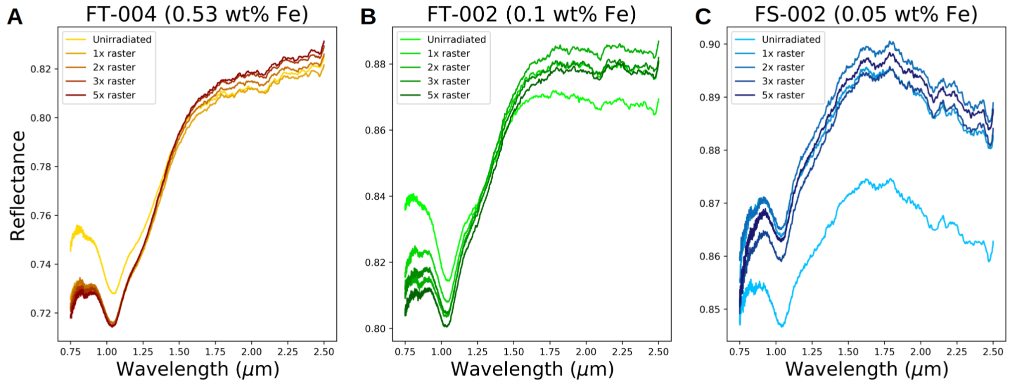

Figure 1: *In situ* near-infrared reflectance spectra of **A.** F-T-004; **B.** F-T-002; **C.** F-S-002 samples when unirradiated and after 1x, 2x, 3x and 5x laser pulses.

after irradiation, which might suggest their vaporization by laser irradiation. This finding is reminiscent of combined laser and ion irradiation experiments on FeS showed segregation and subsequent removal of S to the surface, suggesting SW – especially heating impacts – could be a possible mechanism for S depletion on asteroid Eros [10].

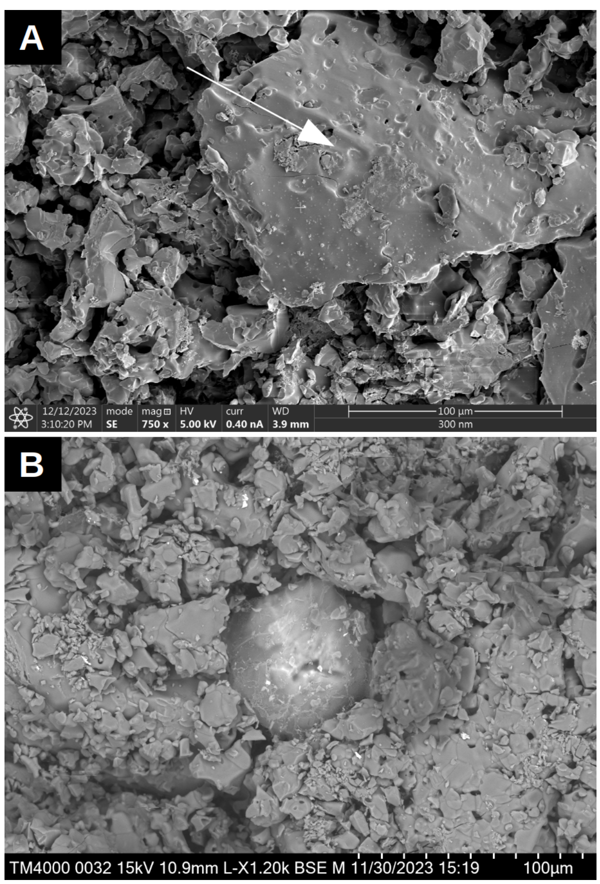

Figure 2: **A.** Secondary electron image of a melt-rich deposit (white arrow) in the F-T-004 sample; **B.** Backscattered electron image of a S-rich deposit in the F-T-004 sample.

We prepared FIB sections for both melt-rich and S-rich regions of our samples for analysis in the TEM. The analyses are ongoing. We expect to observe melt layers with similar thicknesses (50-100 nm) to those seen in our samples mixed with graphite, as well as thin S-rich deposits on top of the crystalline phase.

Conclusion: The initial analyses of our laser irradiation experiments indicate that SW – and in particular micrometeoroid bombardment, alters the optical, morphological, microstructural and chemical characteristics of S-rich Mercury analogs, as it does for other analogs previously studied [13]. The spectral modifications due to laser irradiation exhibit a change in spectral regime at very low Fe content, reinforcing that surface composition is an essential parameter to study SW. We observed both well-known SW characteristics (reddening of infrared reflectance spectra, formation of melt-rich deposits) and new features (sulfur-rich deposits).

We aim to investigate the Si wafers, looking for any ejected S-rich material susceptible to further corroborating a S depletion of our samples due to laser irradiation. We are also investigating the effects of solar wind irradiation on the microstructural, chemical, and spectral characteristics of Mercury analogs using H^+ and He^+ ion-irradiated samples.

References: [1] Pieters C.M., and Noble S.M. (2016) *JGR-Planets*, *121*, 1865-1884. [2] Lantz C. et al. (2017) *Icarus, 285*, 43-57. [3] Cintala M.J. (1992) *JGR-Planets*, *97*, 947-973. [4] Nittler L.R. et al. (2011) *Science*, *333*, 1847-1850. [5] Weider S.Z. et al. (2015) *E&PSL*, 416, 109-120. [6] Blewett D.T. et al. (2013) *JGR-Planets*, 118, 1013-1032. [7] Blewett D.T. et al. (2018) in *Mercury: The View after MESSENGER*, ed. S.C. Solomon et al. (UK: Cambridge Univ. Press). [8] Evans L.G. et al. (2012) *JGR*, 117. [9] Rodriguez J.A.P. et al. (2023) *PSJ*, 4, 219. [10] Loeffler M.J. et al. (2008) *Icarus*, 195, 622-629. [11] Renggli C.J. et al. (2022) *E&PSL*, 593. [12] Thompson M.S. et al. (2021) *LPSC LII*, Abstract #2548. [13] Bott et al. (2023) *MetSoc 2023*, abstract #6224.